JOURNAL OF BACTERIOLOGY, Feb. 2002, p. 962–970 Vol. 184, No. 4
0021-9193/02/$04.00+0 DOI: 10.1128/JB.184.4.962–970.2002

A Turquoise Mutant Genetically Separates Expression of Genes Encoding Phycoerythrin and Its Associated Linker Peptides

Laura Ort Seib and David M. Kehoe*

Department of Biology, Indiana University, Bloomington, Indiana 47405

Received 21 August 2001/Accepted 5 November 2001

During complementary chromatic adaptation (CCA), cyanobacterial light harvesting structures called phycobilisomes are restructured in response to ambient light quality shifts. Transcription of genes encoding components of the phycobilisome is differentially regulated during this process: red light activates *cpcB2A2*, whereas green light coordinately activates the *cpeCDE* and *cpeBA* operons. Three signal transduction components that regulate CCA have been isolated to date: a sensor-photoreceptor (RcaE) and two response regulators (RcaF and RcaC). Mutations in the genes encoding these components affect the accumulation of both *cpcB2A2* and *cpeBA* gene products. We have isolated and characterized a new pigmentation mutant called Turquoise 1. We demonstrate that this mutant phenotype is due to a dramatic decrease in *cpeBA* transcript abundance and results from a lesion in the *cpeR* gene. However, in this mutant *cpeCDE* RNA levels remain near those found in wild-type cells. Our results show that the coordinate regulation of *cpeBA* and *cpeCDE* by green light can be uncoupled by the loss of CpeR, and we furnish the first genetic evidence that different regulatory mechanisms control these two operons. Sequence analysis of CpeR reveals that it shares limited sequence similarity to members of the PP2C class of protein serine/threonine phosphatases. We also demonstrate that *cpeBA* and *cpeCDE* retain light quality responsiveness in a mutant lacking the RcaE photoreceptor. This provides compelling evidence for the partial control of CCA through an as-yet-uncharacterized second light quality sensing system.

Photosynthetic organisms closely regulate the composition of their light harvesting structures to maximize their photosynthetic efficiency. Much of this control is exerted through regulation of genes encoding light harvesting components. Cyanobacteria and eukaryotic red algae use macromolecular complexes called phycobilisomes (PBS) to capture light energy for photosynthesis (5, 6). PBS consist of light absorbing, chromophorylated phycobiliproteins, and nonchromophorylated, structural peptides termed linkers. PBS are composed of two domains; each contains both phycobiliproteins and linkers. The compact inner region, the core, anchors the PBS to the photosynthetic thylakoid membrane and transmits light energy to the photosynthetic reaction centers. The outer region is made up of structures called rods, which project from the core and harvest light energy.

PBS composition is regulated by numerous environmental factors, including light intensity and, in some species of cyanobacteria, light color. The PBS structural changes that occur in response to changes in the color of ambient light are termed complementary chromatic adaptation (CCA) (8, 9, 43). Most of our understanding of CCA and its regulation has come from the study of the filamentous cyanobacterium *Fremyella diplosiphon* (*Calothrix* sp. strain PCC 7601).

During CCA in *F. diplosiphon*, the composition of the PBS rods is dramatically altered, while the core remains essentially unchanged. CCA, a photoreversible process, is maximally responsive to red light (RL, ~650 nm) and green light (GL, ~540 nm) (19, 23, 46). In RL the rods are composed primarily of the phycobiliprotein phycocyanin (PC; maximum absorbance wavelength, ~620 nm) and its associated linkers, whereas in GL rods contain primarily the phycobiliprotein phycoerythrin (PE; maximum absorbance wavelength, ~566 nm) and its associated linkers. Thus, CCA allows the organism to maximally absorb the predominant ambient wavelength of light and maintain photosynthetic rates at relatively high levels under a range of light qualities (10). During CCA, PBS composition is controlled primarily via transcriptional regulation of three operons encoding PBS structural components (16, 20, 29, 31, 33, 34). *cpeBA*, encoding PE, and *cpeCDE*, encoding the PE linkers, are activated in GL and inactivated in RL. *cpcB2A2H2I2D2* (abbreviated as *cpcB2A2*), which encodes both the RL-inducible PC (PC_i) (*B2A2*) and its associated linkers (*H2I2D2*), is activated in RL and inactivated in GL.

Molecular genetic approaches were used to isolate three genes encoding CCA signal transduction pathway components: *rcaE*, *rcaF*, and *rcaC* (12, 25, 26). RcaE is a member of the sensor class, and RcaF and RcaC are members of the response regulator class of two-component regulatory systems. RcaE covalently binds a bilin chromophore and is a photoreceptor that controls, either by itself or as part of a complex, light quality sensing during CCA (K. Terauchi and D. M. Kehoe, unpublished data). *rcaE* null mutants are phenotypically greenish black and are called black (FdBk) mutants. In FdBk mutants, PE and PC levels are approximately equal (as measured by light absorption), regardless of the ambient light quality (25). *rcaE*, *rcaF*, and *rcaC* have been proposed to encode components that regulate both *cpeBA* and *cpcB2A2*, since lesions in genes encoding these proteins affect both PC_i and PE accumulation (25, 26).

There also appear to be unique mechanisms regulating

* Corresponding author. Mailing address: Department of Biology, Indiana University, 1001 East 3rd St., Bloomington, IN 47405. Phone: (812) 856-4715. Fax: (812) 855-6705. E-mail: dkehoe@bio.indiana.edu.

cpcB2A2 and *cpeBA* during CCA. Such evidence has been supplied by protein synthesis inhibitor experiments, fluence response studies, and analyses of the kinetics of RNA accumulation for these two operons (33, 34, 35). Support for this possibility has also been provided by isolation of *F. diplosiphon* green (FdG) mutants (7, 14, 24, 44). FdG mutants properly regulate PC levels under all light conditions but never accumulate measurable levels of PE. Although such mutants could result from mutations in the PE-specific portion of the CCA regulatory pathway, mutations in many other genes could also lead to this phenotype, since the abundance of PE is controlled by numerous environmental parameters and cellular processes, such as chromophore biosynthesis (24).

cpeBA and *cpeCDE* are not closely linked in the genome (20). However, similar RNA accumulation kinetics have been measured for these two operons in wild-type (WT) cells shifted between RL and GL (20). A central question in the study of CCA is how the expression patterns of *cpeBA* and *cpeCDE* are coordinated. Functional studies to identify light responsive elements in the *cpeBA* or *cpeCDE* promoter have not been reported to date. However, *cpeBA* promoter binding studies have led to the identification of several DNA-binding proteins: RcaA, RcaB, and PepB (40, 42). DNA footprint analyses demonstrated that RcaA and PepB both protect the region from positions −67 to −45 of the *cpeBA* promoter, suggesting that these are the same protein. However, PepB binding activity was equivalent in extracts from both GL- and RL-grown cells (40), whereas RcaA binding was only evident in protein extracts from cells grown in GL (42). The reason for this difference has not yet been resolved. The region from −67 to −45 of the *cpeBA* promoter contains a direct hexameric repeat (5′-TTGTTA-3′) separated by four nucleotides. This direct repeat is not present in the promoter region of *cpeCDE* (42), although it has been identified in a modified form with five of the six nucleotides conserved, the repeats separated by 52 bp, and in the opposite orientation relative to their position in *cpeBA* (40). There is also a conserved 17-bp sequence present upstream of both operons (20). It is 83 bp 5′ of the *cpeBA* transcription start site, and its reverse complement is 195 bp 5′ of the *cpeCDE* transcription start site. The role of this sequence is unclear, although a repeated sequence found within this element has been noted to be quite common in the genome of this organism (32). Overall, the mechanism through which coordinated light regulation of *cpeBA* and *cpeCDE* is achieved remains unclear.

In this report we analyze a member of a new class of *F. diplosiphon* pigmentation mutants, the Turquoise 1 (FdTq1) mutant. We demonstrate that in this genetic background the patterns of *cpeBA* and *cpeCDE* transcript accumulation have been altered and that these operons are no longer coordinately regulated. In addition, we have cloned, sequenced, and analyzed the gene responsible for the FdTq1 mutant phenotype. Our results suggest a possible mechanism through which *cpeBA* expression may, in part, be regulated.

MATERIALS AND METHODS

Growth and transformation. Our *F. diplosiphon* WT is a shortened filament strain called Fd33 (originally SF33) (15). The FdBk mutant used here has been previously described (25). Strains were grown in BG-11 medium (1) with 10 mM HEPES (pH 8.0), either with or without 25 μg of kanamycin per ml (kan_{25}) at 25 to 30°C. Liquid cultures were bubbled with air containing 3% CO_2 while illuminated with 15 μmol of either red (Industrial F20T12/R; Lightbulbs Unlimited, Pomano Beach, Fla.) or green (General Electric F20T12-G) fluorescent light m^{-2} s^{-1}. Growth was monitored and cell densities were normalized at an absorption wavelength of 750 nm (A_{750}) by using a Beckman DU640B spectrophotometer. Plated cultures were grown in 40 μmol of cool white fluorescent light (General Electric F20T12-CW) m^{-2} s^{-1}. Photon flux was measured with a Li-Cor LI-250 light meter connected to a LI109SA Quantum Sensor. Transformations were conducted by electroporation by using previously described methods (27).

FdTq1 mutant isolation and complementation. FdTq1 was isolated as a spontaneous *F. diplosiphon* pigmentation mutant growing on an FdBk mutant plate. FdTq1 was complemented by transformation with an *F. diplosiphon* WT genomic plasmid library (27). Transformants were screened on plates containing kan_{25} for colonies with a restored FdBk phenotype. To establish whether the FdBk phenotype of these colonies was due to the introduced plasmid or a secondary mutation, cells were plated onto BG-11 with or without kan_{25} and examined for reversion. Plasmids were rescued from phenotypically complemented *F. diplosiphon* lines by extraction of total DNA, transformation into *Escherichia coli* DH5α, and selection for resistant colonies on Luria-Bertani plates (38) containing kan_{25}.

DNA cloning, sequencing, and analysis. *Escherichia coli* rescued plasmids were isolated by using a Qiaprep Miniprep kit (Qiagen, Valencia, Calif.). PCR amplifications were carried out using the Expand PCR Kit (Roche, Nutley, N.J.) with an MJ Research PTC-150 MiniCycler. Primers used in PCR amplifications to check for insertions in the regions containing *cpeBA*, *cpeCDE*, and *cpeYZ* (encoding the putative lyases for PE [24]) in the FdTq1 mutant were as follows: for *cpeBA* and *cpeYZ* (checked together), 5′-AGCCTGCTCC TTTCTCTAAT GG-3′ (hybridizes to the noncoding strand 365 bp upstream of the start of translation of *cpeB* [20]) and 5′-CCGCTGAAAC TTCGTTGTCA TTT-3′ (hybridizes to the coding strand 12 bp upstream of the end of *cpeZ* translation [31]); for *cpeCDE*, 5′-CCATTACCCA ATTTCCCATG CC-3′ (hybridizes to the noncoding strand 290 bp upstream of the start of translation of *cpeC* [20]) and 5′-GCTTATCTGA ACCGTATTGC CAT-3′ (hybridizes to the coding strand 33 bp downstream of the end of *cpeE* [21]).

Primers used for subcloning *trqA*, along with the DNA region upstream of open reading frame (ORF) 3, into pPL2.7 were as follows: BPCR1P, 5′-GCGCTGCAGT CAAGTCATAT AGATACAAAC TCA-3′; BPCR1K, 5′-GTGCTGCAGG CTT AATCCAA CCTACATCTG C-3′; BPCR2K, 5′-CTAGGTACCG TGTGGGT AAG CCTAGATAAA GGTAT-3′; and APCR1P, 5′-CACGGTACCT AGGGTC ATAA CTAGATGAGG ATAAA-3′. Primers BPCR1P and BPCR1K were used to PCR amplify the intergenic region upstream of ORF 3, and BPCR2K and APCR1P were used to amplify *trqA*. Primers ending with "P" had a *Pst*I site at their 5′ ends, and those ending with K had a *Kpn*I site at their 5′ ends. PCR products were combined and annealed at the *Kpn*I site and then reamplified with BPCR1P and APCR1P. The resulting PCR product was cut with *Pst*I and inserted into the *Pst*I site of the shuttle plasmid pPL2.7 (13, 39). Sequencing of this subcloned region, and all other sequencing, was conducted by using an ABI Big Dye sequencing kit and an ABI Prism 3700 automated sequencer (Applied Biosystems, Foster City, Calif.). Database searches were carried out by using the PSI BLAST (2) and BLASTP (3) network services at the National Center for Biotechnology Information. Sequence alignments were performed by using both BLASTP (3) and CLUSTAL W (http://www2.ebi.ac.uk/clustalw).

The region of genomic DNA upstream of *trqA* was isolated by using a PCR-based approach. PCR amplifications were performed with an *F. diplosiphon* WT genomic plasmid library in pPL2.7 (27). Two sets of primers were used: primers that annealed to vector sequence near the genomic DNA insertion site (3′ end of the primer toward the insertion) and primers that annealed to the coding strand or sequences upstream of *trqA*. The pPL2.7 primers also each contained sequence corresponding to a *Bam*HI site at their 5′ ends; their sequences were 5′-CGGGATCCCT GCCAGAATTC GCCCCTCT-3′ and 5′-CGGGATCCCT TGCCATCCTA TGGAACTGC-3′. The primers specific for the *trqA* region were 5′-GCGCTGCAGT TAGAGGCAGA TTCGGCAGGG-3′, 5′-GCATAG GTTT CCAGGTTCAA CA-3′, 5′-CCCAAGACTA TACTTTCGGC AA-3′, 5′-CGTAAGCGGT GACTAACACA AA-3′, 5′-ACATAAGTCA ATCACTG CTG GAT-3′, and 5′-GGACATTTAG TGGGGTAGGC A-3′. These primers were also used for sequencing of this region. Reactions were separated on 0.8% agarose TAE gels, and bands containing amplified fragments were excised, purified, and sequenced.

PCR amplifications of the *rcaE* or *rcaF* locus in WT and the FdBk mutant were carried out with primer EC100 (5′-ACGTGAGCTC GGATCCCAGA ACACC TCACC ATTCGGT-3′), which anneals ca. 500 bp upstream of the first methionine in *rcaE* and encodes a *Bam*HI and *Sac*I site at its 5′ end, and primer RCAF-SP2 (5′-CCAATGGAGA ATTCTACTTA TTTG-3′), which anneals to

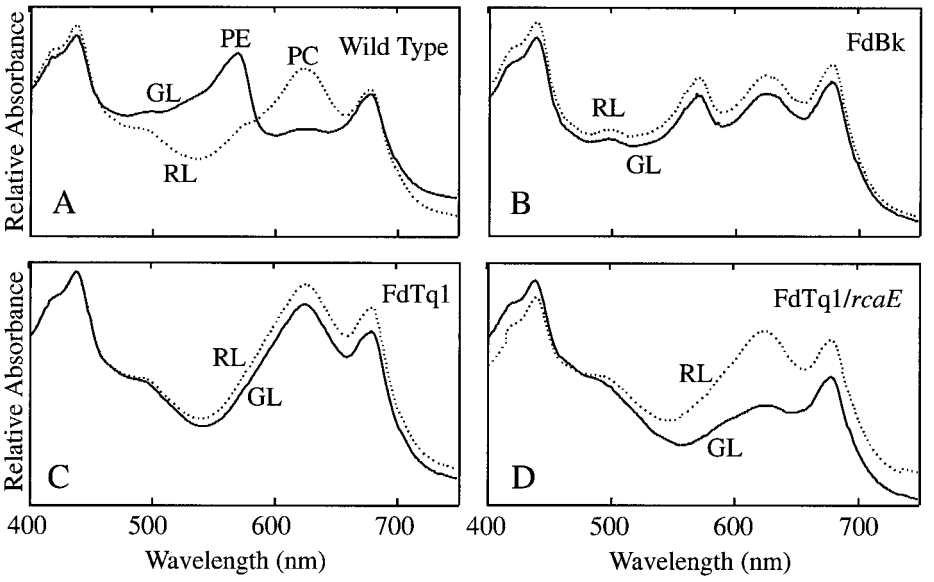

FIG. 1. Absorption spectra of *F. diplosiphon* cells grown in liquid BG-11 in 15 μmol of RL (dashed line) and GL (solid line) m^{-2} s^{-1}. The *x* axis is the wavelength from 400 to 750 nm, and the *y* axis is the relative absorbance. (A) WT cells (B) FdBk mutant cells (C) FdTq1 mutant cells (D) FdTq1 mutant cells transformed with a pDK4, which contains a WT copy of *rcaE*. Chlorophyll absorption peaks are at ca. 430 and 680 nm; PC and PE absorbance peaks are labeled.

the 3′ end of the *rcaF* coding region. Southern blots were conducted according to standard methods (38) by using the PCR products generated with the EC100 and RCAF-SP2 primers.

RNA analysis. RNA was extracted from 50 ml of *F. diplosiphon* liquid cultures at mid-logarithmic-growth phase (A_{750}, ~0.6). Cells were quick cooled to 4°C by swirling in flasks submerged in liquid nitrogen and then centrifuged at 4,000 × *g* at 4°C for 10 min. Cell pellets were pipetted vigorously with 5 ml of Tri-Reagent (Molecular Research Center, Cincinnati, Ohio), and RNA isolation was performed according to the manufacturer's instructions. RNA was separated for Northern analysis by electrophoresis for 2.5 h at 100 V on 1% agarose-formaldehyde gels (38). RNA was transferred overnight from gels to Nytran Plus nylon membranes (Schleicher & Schuell, Keene, N.H.) using 20× SSC (1× SSC is 0.15 M NaCl plus 0.015 M sodium citrate) and then UV cross-linked as recommended by the manufacturer. Gel-purified PCR products were used as probes for *cpeBA* (from −70 to +600, relative to *cpeB* translation start [31]) and *cpeCDE* (from −310 to +928, relative to *cpeC* translation start [20]). Gel-purified restriction fragments were used as probes for *cpcB2A2* (from −250 to +1020 relative to transcription start [17]) and rRNA (the ca. 5-kb *Pst*I/*Eco*RI fragment containing the 23S ribosomal DNA from pAN4 [45]). Probes were labeled with [α-^{32}P]dCTP and purified by passing over Centri-Sep spin columns (Princeton Separations, Adelphia, N.J.). RNA blots were hybridized at 65°C for 15 to 18 h in 10 ml of hybridization buffer (0.1 M NaH_2PO_4, pH 7.0; 0.5 M NaCl; 0.1 M Tris, pH 7.5; 2 mM EDTA; 0.1% sodium dodecyl sulfate [SDS]) and then washed two times for 10 min at 27°C with 50 ml of wash buffer 1 (10 mM NaH_2PO_4, pH 7; 20 mM EDTA; 0.1% SDS), once for 10 min at 50°C with wash buffer 1, and then once for 10 min at 50°C with wash buffer 2 (50 mM NaH_2PO_4, pH 7; 20 mM EDTA; 0.1% SDS). Quantification of probe hybridization was conducted using a Molecular Dynamics SP PhosphorImager. Blots were also exposed to Kodak X-Omat AR film at −80°C with an intensifying screen. Each blot was stripped and rehybridized using the rRNA probe (45). For each lane, the relative ribosomal value obtained from the PhosphorImager was used to normalize the test mRNA value, which was then expressed as a percentage of the WT GL value (for *cpeCDE* and *cpeBA*) or RL value (for *cpcB2A2*). Each result is the mean value of three to four independent experiments. Statistical analyses employed a two-tailed Student's *t* test.

RESULTS

The FdTq1 mutant fails to accumulate PE. In WT cells, PC levels are high in RL and low in GL, while PE levels are low in RL and high in GL (Fig. 1A). In an FdBk mutant, which lacks functional RcaE (Terauchi and Kehoe, unpublished), both PE and PC accumulate to intermediate levels in both RL and GL (Fig. 1B). FdTq1 is a member of a new class of pigmentation mutants that have been generated in an FdBk mutant background and designated Turquoise (FdTq) mutants. Unlike the green-black color of their parent strain, FdTq mutants are blue-green. Whole-cell absorbance spectra taken of FdTq1 demonstrate that it accumulates high levels of PC and no detectable PE in both RL and GL (Fig. 1C). Under all light conditions it appears similar to WT cells grown in RL. The fact that FdTq1 was isolated from a FdBk mutant line suggested that its phenotype was the result of a mutation in a second genetic locus. To test this, the plasmid pDK4 (25), containing a WT copy of *rcaE*, was introduced into FdTq1. Transformed cells were grown in RL and GL and whole-cell absorbance measurements were made. In FdTq1 cells containing WT *rcaE*, light regulation of PC abundance was clearly restored, with levels in RL and GL that appear identical to those observed in WT cells (Fig. 1D). However, these transformed cells did not accumulate any detectable PE in either GL or RL. These results suggested that the FdTq1 phenotype was the result of a secondary mutation in a *rcaE* null mutant background that resulted in the loss of PE accumulation in all light conditions examined. Thus, the phenotype of FdTq1 transformed with pDK4 (Fig. 1D) is equivalent to that of FdG mutants, which appear to exist in an otherwise WT background (7, 14, 24, 44).

All pigmentation mutations thus far complemented for this organism (over 100 total) have resulted from DNA insertion events (12, 24, 25, 26; D. M. Kehoe, unpublished data). Thus, the FdTq1 genes encoding the known PE apoproteins, linkers, lyases (*cpeBA*, *cpeCDE*, and *cpeYZ*), and flanking sequences were checked for mutations caused by DNA insertion events by using PCR amplification. Neither these operons nor their surrounding sequences had DNA insertions (data not shown).

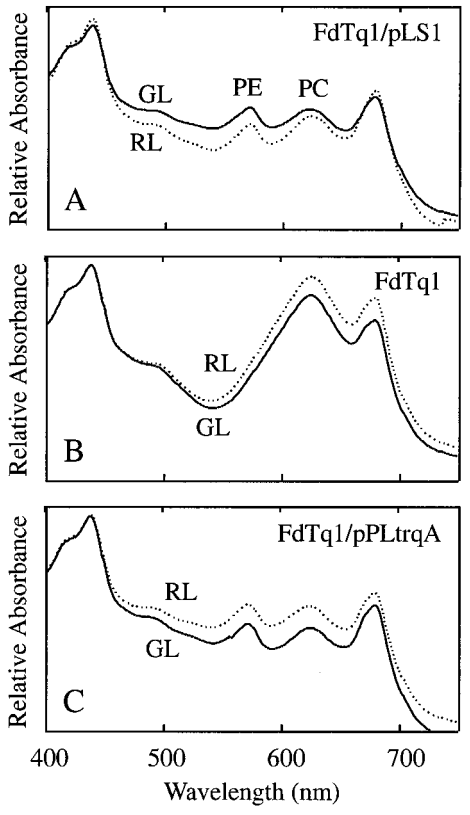

FIG. 2. Complemented FdTq1 mutant absorption spectra. (A) The FdTq1 mutant harboring the pLS1 plasmid was grown in liquid BG-11 containing kan_{25} in 15 μmol of RL (dashed line) and GL (solid line) m^{-2} s^{-1}. (B) The FdTq1 mutant containing pLS1 after 4 days' growth in BG-11 without kan_{25} in 15 μmol of RL (dashed line) and GL (solid line) m^{-2} s^{-1}. (C) The FdTq1 mutant was transformed with pPLtrqA (Fig. 3C) and grown in liquid BG-11 containing kan_{25} in 15 μmol of RL (dashed line) and GL (solid line) m^{-2} s^{-1}. The chlorophyll absorption peaks are at ca. 430 and 680 nm; the PC and PE absorption peaks are labeled.

Complementation of FdTq1. To determine the nature of the secondary mutation, FdTq1 cells were transformed with a WT *F. diplosiphon* genomic DNA plasmid library (27) and spread on plates containing kan_{25}. Approximately 8,000 kan_{25}-resistant transformed colonies were visually screened for a FdBk mutant phenotype. Ten partially or completely black colonies were identified, isolated, and restreaked onto BG-11 plates containing kan_{25}. All of these segregated completely to the FdBk mutant phenotype and, when grown in liquid with kan_{25} selection, had whole-cell absorption spectral profiles (Fig. 2A) that were very similar to that of FdBk (Fig. 1B). All of the transformed lines rapidly reverted back to the FdTq1 phenotype upon removal from kan_{25} selection (Fig. 2B). A plasmid was rescued from one of the transformed lines into *E. coli* and designated pLS1. This plasmid contained a 1.6-kb fragment of *F. diplosiphon* genomic DNA. Reintroduction of purified pLS1 plasmid into FdTq1 conferred the FdBk pigment phenotype (data not shown).

Sequencing and analysis of the pLS1 genomic DNA. Sequencing of the 1.6-kb fragment of *F. diplosiphon* WT genomic DNA within pLS1 revealed ORFs that were initially designated ORF 1, ORF 2A, and ORF 2B (Fig. 3A). The ORF 1 sequence was 336 bp long and was located at one end of the genomic DNA fragment. ORF 2A was 206 bp long and was located 455 bp downstream of, and in the same orientation as, ORF 1. ORF 2B was 189 bp long, in the same orientation and reading frame as ORF 2A, and separated from ORF 2A by a single stop codon. The corresponding 1.6-kb region of genomic DNA was examined in the FdTq1 mutant and compared to the WT fragment. Only a single difference was identified: the FdTq1 sequence contained a 1.5-kb DNA insertion in ORF 1, 42 bp from its 3′ end (between the 15th and 14th amino acids from the carboxyl terminus) (Fig. 3A). ORF 1 was given the designation *trqA* based on this result.

The 5′ end and upstream regions of *trqA* were not apparent in the genomic DNA insert of pLS1. To obtain sequence corresponding to this region, PCR amplification of clones within the *F. diplosiphon* WT genomic plasmid library was conducted with one primer that annealed to the noncoding strand near the 5′ end of *trqA* and another annealed to one of two sites within the pPL2.7 shuttle plasmid near the genomic DNA insertion site. The PCR products generated were sequenced directly. This approach provided ca. 1.6 kb of sequence upstream of the 5′ end of *trqA* found in pLS1. Assuming the first methionine is used during translation, 24 bp (encoding eight amino acids) of the 5′ end of *trqA* was absent in the genomic DNA found in pLS1. Three additional ORFs (ORF 3, ORF 4, and ORF 5) were found upstream of *trqA* (Fig. 3B); the 3′ end of ORF 3 overlapped the 5′ end of *trqA* for 23 bp. ORF 4 and ORF 3 are separated by 308 bp, if we assume that the first methionine of ORF 3 is the translation start site.

To conclusively establish whether the insertion in *trqA* caused the FdTq1 mutant phenotype, *trqA* alone was introduced into FdTq1 mutant cells. We wanted to include the promoter of *trqA*, but because its coding region overlapped that of ORF 3 it was not possible to clearly define such a region immediately upstream of *trqA*. Both the size and expression level of *trqA* RNA in RL and GL were investigated by using Northern blots, but no transcript corresponding to *trqA* could be detected (data not shown). Thus, a 292-bp region between ORF 3 and ORF 4 was inserted upstream of *trqA* (Fig. 3B) since it represented the most likely promoter region for both ORF 3 and *trqA*. All of the ORF 3 coding sequence was removed except the last 120 bp. This chimera was then cloned into the *Pst*I site of pPL2.7 (13) to make pPLtrqA (Fig. 3C) and transformed into FdTq1. The phenotype of FdTq1 transformed with pPLtrqA (Fig. 2C) was identical to that of the mutant complemented with pLS1 (Fig. 2A). This result, and the presence of a DNA insertion at the 3′ end of *trqA* in FdTq1, leads us to conclude that the mutation in *trqA* is the secondary mutation in the FdBk mutant that caused the FdTq1 mutant phenotype.

BLASTP searches (3) were conducted for the five ORFs described above. No perfect sequence matches were found in GenBank for ORFs 1 to 4 when they were originally analyzed. However, analysis of ORF 5, which was sequenced last, demonstrated that it was *cpeE* (100% identity), which is located at the 3′ end of the *cpeCDE* operon and encodes a PE linker peptide (21). Our subsequent BLASTP searches by using ORFs 1 to 4 showed that the sequences of ORF 4, ORF 3, and *trqA* (and their corresponding proteins) had been submitted to GenBank in the intervening period as *cpeS* (CpeS), *cpeT* (CpeT), and *cpeR*

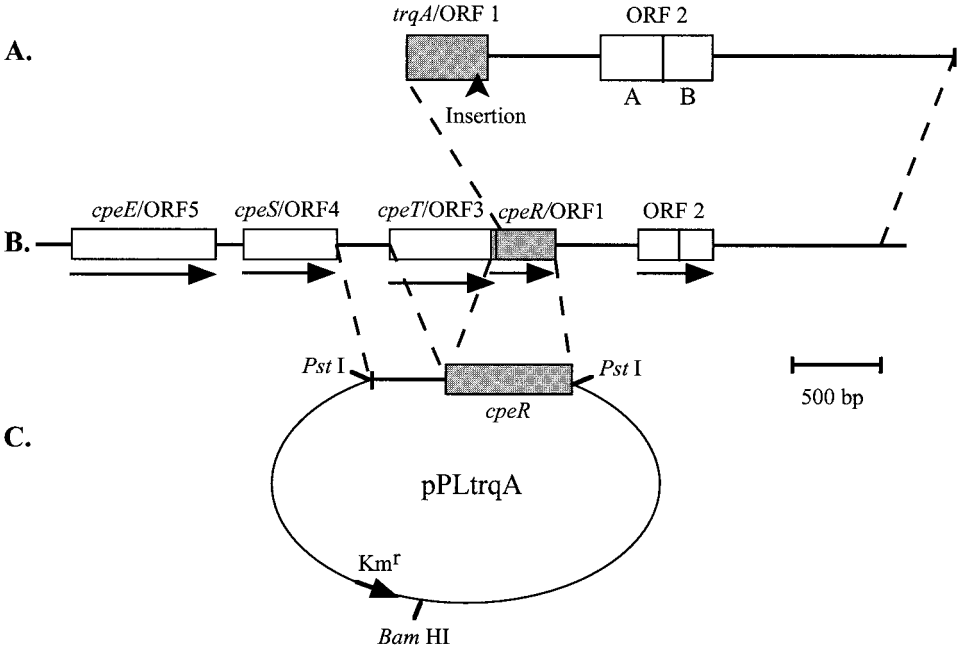

FIG. 3. Genomic DNA fragments used for complementation of the FdTq1 mutant. (A) The *F. diplosiphon* genomic DNA fragment contained within pLS1 contained a 5′ truncated form of *trqA*/ORF 1 and ORFs 2A and 2B. The location of a ca. 1.5-kb DNA insertion within *trqA*/ORF 1 is shown. (B) The region of the *F. diplosiphon* genome containing the pLS1 insert DNA (indicated by dashed lines). ORF numbers and GenBank designations (accession no. AF334109) are provided above each ORF, and the direction of transcription is indicated by an arrow for each. The *cpeT*/ORF 3 and *cpeR*/ORF 1 reading frames overlap. *cpeE*/OFR 5 is located at the 3′ end of the *cpeCDE* operon. (C) Construction of a plasmid containing *cpeR* fused to the putative promoter sequence upstream of *cpeT*. This chimera (indicated by dashed lines) was cloned into the unique *Pst*I site of pPL2.7 to make pPLtrqA, which was then transformed into the FdTq mutant.

(CpeR) (accession no. AF334109 [unpublished], 100% identity for each) (Fig. 3B). Thus, *trqA* is *cpeR*. ORF 2A had also been submitted to GenBank, as an unknown protein (accession no. AF334109 [unpublished]). BLASTP searches using the combined ORF 2A and ORF 2B translated sequences demonstrated that this region was closely related to the *crtE* gene product geranylgeranyl diphosphate synthase in the thermophilic cyanobacterium *Synechococcus elongatus* (accession no. AB016093; expectation [E] value of 6×10^{-37}) (36).

A BLASTP analysis of the translated protein sequence of CpeR provided the most significant alignment to a putative protein phosphatase from *Mycoplasma genitalium* (accession no. NP__072770 [22]). Additional searches were conducted by using CpeR and PSI-BLAST (2). After the second PSI-BLAST iteration, only three sequences other than CpeR itself produced alignments with an E value at or below 5×10^{-6}. All of these were putative protein phosphatases from microorganisms; two of the three were categorized as PP2C class protein serine/threonine phosphatases. The alignment of these sequences with CpeR is shown in Fig. 4. CpeR, from amino acids 47 to 102, was 32% identical and 53% similar to the *M. genitalium* putative protein phosphatase after the second PSI-BLAST iteration.

The CpeR sequence, starting from the first methionine, was also analyzed by using various proteomics tools at the ExPASy Molecular Biology Server (http://www.expasy.ch/) and the San Diego Supercomputing Center's Biology WorkBench (http://workbench.sdsc.edu/). CpeR is composed of 120 amino acids and has an estimated molecular mass of 13.8 kDa with a theoretical pI of 9.2. InterPro Scan (http://www.ebi.ac.uk/interpro/scan.html) detected no significant similarities to CpeR in PROSITE, Pfam, or PRINTS domain databases. Both SAPS and GREASE (Kyte-Doolittle Hydropathy Profile) programs found that CpeR contained predominantly hydrophilic residues and no obvious potential membrane-spanning domains, clusters of positively or negatively charged residues, or large hydrophobic regions. The PELE protein structure prediction program identified three short regions (5 to 20 amino acids) of potential α-helices, and three possible β-strand stretches (5 to 10 amino acids) within CpeR. The majority of the protein was designated as random coil in this analysis. Finally, the HTH Program was unable to predict any helix-turn-helix motifs in CpeR.

CpeR is required for expression of *cpeBA* but not *cpeCDE*. By using Northern blots, the effect of the *cpeR* mutation on transcript accumulation patterns in RL and GL was measured for *cpeBA*, *cpeCDE*, and *cpcB2A2* (Fig. 5A). RNA was isolated from three lines (WT, an FdBk mutant, and the FdTq1 mutant) grown under each light condition. Three to four independent RNA isolations and hybridizations were conducted for each operon and all values were normalized by using ribosomal loading control values.

The expression of *cpeBA* in WT cells was 45 times higher in GL than in RL, but *cpeBA* RNA was not detected in RL or GL in the FdTq1 mutant (Fig. 5B). This finding is consistent with the pigmentation phenotypes of FdTq1 observed under these two light conditions (Fig. 1C). Surprisingly, for *cpeBA* in the FdBk mutant, some residual regulation by light quality remained: RNA levels in GL-grown cells were still 2.9-fold higher than in RL-grown cells ($0.05 > P > 0.02$). These data

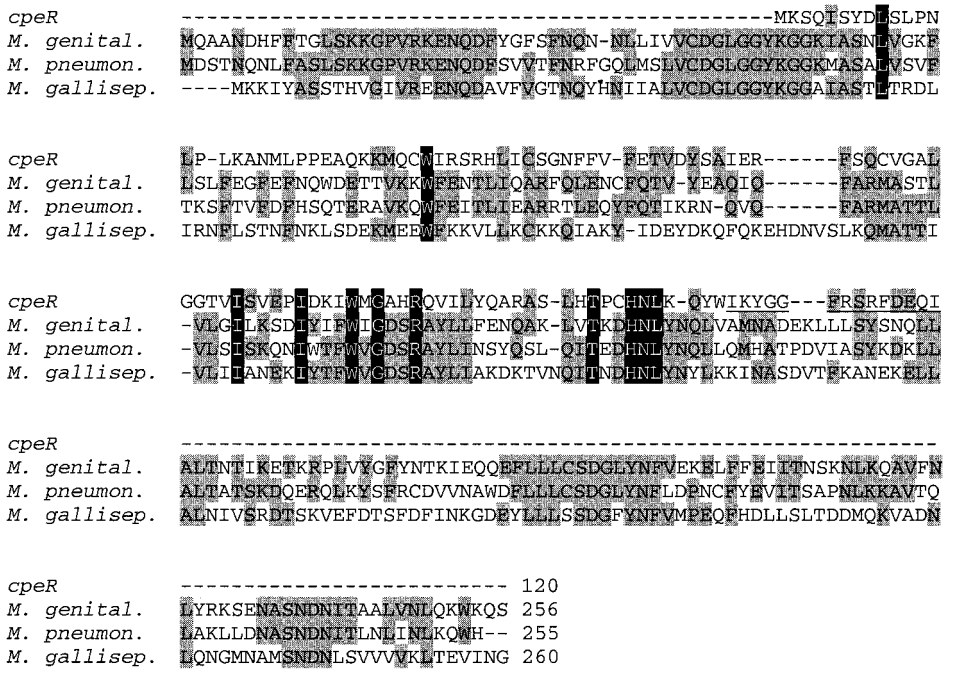

FIG. 4. Similarity of *cpeR* to PP2C class protein serine/threonine phosphatases from three bacterial *Mycoplasma* species: *M. genital*., *M. genitalium* putative protein phosphatase (accession no. NP_072770.1); *M. pneumon*., *M. pneumoniae* protein phosphatase 2C homolog (accession no. NP_109935.1); and *M. gallisep*., *M. gallisepticum* putative protein phosphatase (accession no. AAF36762.1). Alignment was performed with the CLUSTALW program with minor realignments made by using information from a PSI-BLAST analysis (second iteration). Residues conserved between two or three species are shown in gray; residues conserved in all four proteins are highlighted in black. Gaps (represented by dashes) have been inserted to maximize alignments. Total number of amino acids in each of the proteins is provided. Underlined amino acids in *cpeR* are those encoded downstream of the site of the DNA insertion in FdTq1.

suggest that RcaE is exerting its control under both light conditions since, compared to the WT, *cpeBA* in the FdBk mutant appeared to be both less silenced in RL and less activated in GL. Since *F. diplosiphon* contains approximately six chromosomal copies per cell, PCR amplification and Southern blot analysis of the genomic region containing *rcaE* in the FdBk mutant were conducted to insure that no WT copies of the gene remained. Because a DNA insertion 69 bp downstream of the putative RcaE translation start site caused the *rcaE* mutation (K. Terauchi, A. R. Grossman, and D. M. Kehoe, unpublished data), this polymorphism is easily detected. Neither method detected any WT-size *rcaE* in this mutant (Fig. 6).

The *cpeCDE* RNA level was 10.5 times higher in GL than in RL in WT cells (Fig. 5C). A portion of the WT level of RL and GL regulation of expression was also retained for this operon in the FdBk mutant. However, the non-RcaE-based light-sensing system(s) clearly contributed much more to the control of RL and GL responsiveness for *cpeCDE* than for *cpeBA*, since for this operon a 7.8-fold difference in transcript accumulation between the two light conditions remained in the FdBk mutant (Fig. 5C) ($0.05 > P > 0.02$). Measurement of *cpeCDE* transcript levels in FdTq1 highlighted a second major difference between the regulation mechanisms of these two operons. In this mutant, *cpeCDE* transcript was still 3.8-fold more abundant in GL than RL and accumulated to levels similar to those measured in FdBk cells (Fig. 5C). These results unambiguously demonstrate that, although CpeR is absolutely required for the expression of *cpeBA* in both RL and GL, it plays no obvious role in regulating *cpeCDE* expression in GL and a minor role, if any, in RL ($P > 0.05$ for significance of the difference between the means for *cpeCDE* levels in FdBk and FdTq1 mutant cells grown in RL).

For *cpcB2A2* in WT cells, the RL expression level was ca. 10 times that measured for GL (Fig. 5D). FdBk mutant cells had no statistically significant difference in *cpcB2A2* RNA levels when grown in RL and GL ($P \gg 0.5$), and both levels were between 55 and 65% of the WT level in RL. This operon also continued to be expressed in the FdTq1 mutant but, as in the FdBk mutant, was not differentially regulated in RL and GL.

DISCUSSION

In this report we describe the isolation, characterization, and complementation of FdTq1, the first member of a newly described class of turquoise-colored *F. diplosiphon* mutants that were generated in an FdBk mutant background. Its color phenotype is novel, since it is equivalent to that of WT cells grown in RL (Fig. 1A) but is not altered by changes in light quality (Fig. 1C). By introducing plasmid-borne WT *rcaE* into this mutant, we have demonstrated that in a WT background, FdTq1 is phenotypically equivalent to the previously described FdG mutant class (7, 14, 24, 44), in which PC expression is normal but PE fails to accumulate in either RL or GL (Fig. 1D). Although many FdG mutants have been isolated, the only one that has been complemented to date was found to contain a lesion in the *cpeYZ* operon, which appears to encode subunits of a PE lyase (24).

We were able to complement FdTq1 with *trqA* (Fig. 2C), and

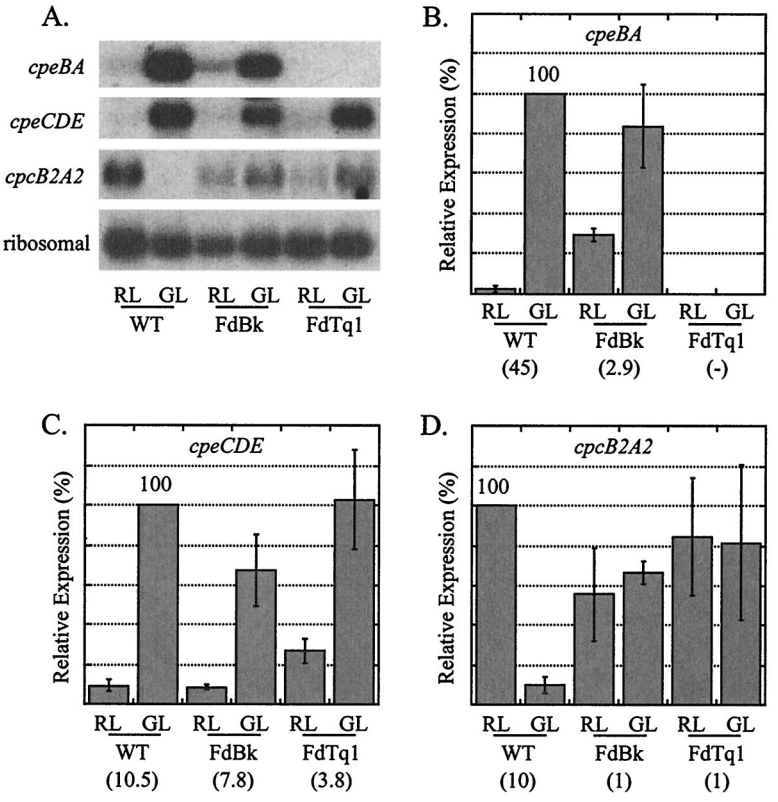

FIG. 5. Northern blot analysis of *cpeBA*, *cpeCDE*, and *cpcB2A2* expression in WT, the FdBk mutant, and the FdTq1 mutant. (A) Representative autoradiograms of the data presented in panels B to D showing hybridization to the probes listed on the left. RNA was isolated from the WT and the two mutant lines after growth in 15 μmol of RL and GL m^{-2} s^{-1}. (B) Mean values from four independent experiments of *cpeBA* RNA, expressed as a percentage of the WT GL value (set to 100%). (C) Mean values from three independent experiments of *cpeCDE* RNA, expressed as a percentage of the WT GL value (set to 100%). (D) Mean values from four independent experiments of *cpcB2A2* RNA, expressed as a percentage of the WT RL value (set to 100%). The numbers in parentheses are the fold induction between RL and GL for each operon in each cell line. Standard errors are shown; *P* values are provided in the text. Measurements were normalized by using ribosomal values prior to calculation of means.

we found a large DNA insertion in the 3′ end of *trqA* in the FdTq1 mutant (Fig. 3A). These data demonstrate that the lesion in *trqA* is responsible for the shift from a FdBk mutant to the FdTq mutant phenotype. Although the amino-terminal eight amino acids of the putative protein encoded by *trqA* were not encoded by the *F. diplosiphon* genomic DNA in pLS1, this plasmid still complemented FdTq1. The most likely reasons for this are (i) that these residues are not required for protein function, (ii) that the truncated protein functions suboptimally but still complements FdTq1 in our assay, or (iii) that the translation start site is actually within the sequence contained in pLS1.

BLAST searches with *trqA* and the surrounding ORFs revealed that this region of the genome lies just downstream of the *cpeCDE* operon (Fig. 3B). Since the sequences of the ORFs in this region have been submitted to GenBank (accession no. AF334109), the designation *cpeR* supplants the name *trqA*. CpeR is most similar to a putative member of the PP2C class of protein phosphatases (22), which dephosphorylate serine and threonine residues and are found in both eukaryotes and prokaryotes (4, 18, 41). CpeR was most similar to the β5-β8 strand region of known protein phosphatases (18). However, the predicted size of CpeR is much smaller than previously described PP2C class proteins and it lacks most of the catalytic site and residues necessary for PP2C function (Fig. 4) (18). Thus, it is unlikely that, at least by itself, CpeR acts as a phosphatase and its function remains to be determined. It is also unclear whether CpeR is an element of the CCA or some other regulatory pathway. The three CCA signal transduction components isolated to date suggest that a two-component regulatory system makes up at least the initial part of this regulatory pathway (12, 25, 26). These pathways are typically regulated by histidine-aspartate phosphotransfer reactions. It is possible that CpeR acts in the downstream portion of this pathway, since two-component systems have been found to be integrated with mitogen-activated protein kinase pathways in both yeast and *Arabidopsis* (11, 28, 30, 37). The activities of two binding proteins that interact with the *cpeBA* promoter have been either shown (RcaA) or suggested (PepB) to be modified by their phosphorylation state (40, 42). Thus, the possibility that CpeR, in conjunction with one or more other factors, dephosphorylates a component(s) in the *cpeBA*-specific portion of the CCA pathway is an interesting one. Other than identifying relatively weak similarity to PP2C class proteins (Fig. 4), our analysis of the CpeR sequence failed to identify any outstanding features that might provide clues regarding its function. It appears to be primarily hydrophilic, possesses no obvious transmembrane stretches, and contains two to three potential α-helical sequences and the same number of β-strand-forming regions. It has no obvious helix-turn-

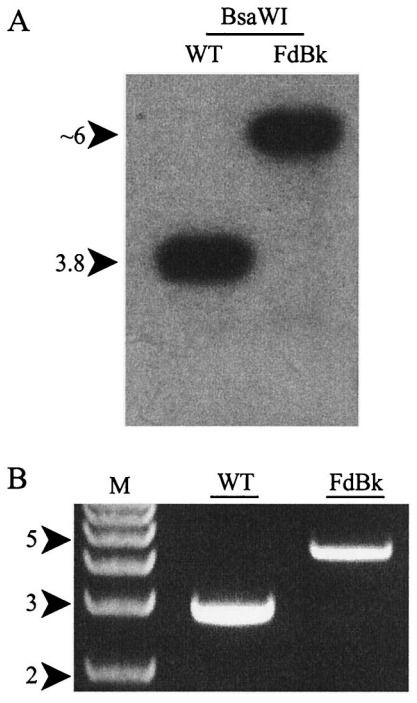

FIG. 6. Check of the FdBk mutant for WT copies of *rcaE*. (A) Autoradiogram of a Southern blot of genomic WT or FdBk DNA cut with *Bsa*W1 and hybridized with an *rcaE* probe. The DNA insertion in *rcaE* in the FdBk mutant results in decreased mobility that is distinguishable from the mobility of the same region in WT. (B) PCR amplification and agarose gel electrophoresis were used to examine the size of the *rcaE* region in the genome of the WT and the FdBk mutant.

helix motifs, which often serve as DNA-binding domains in transcription factors.

Since the DNA insertion in *cpeR* in the FdTq1 mutant effectively ends CpeR only 14 amino acids from its carboxyl terminus, it is possible that FdTq1 cells contain a modified form of CpeR. If so, it appears to be functionally incapable of contributing to *cpeBA* expression. This insertion site may be in a critical region of the protein, since it is only four amino acids away from a block of three amino acids that are absolutely conserved in the three proteins with greatest similarity to CpeR (Fig. 4).

The disruption of *cpeR* had no significant effect on *cpcB2A2* expression (Fig. 5D) but led to the failure to accumulate measurable levels of *cpeBA* RNA, which provides an explanation for the lack of accumulation of functional PE in these cells (Fig. 5B). *cpeCDE* transcript levels in FdTq1, however, were actually slightly higher than those measured in the FdBk mutant and WT backgrounds (Fig. 5C). Thus, CpeR is required for normal *cpeBA* expression but exerts little or no control over the accumulation of *cpeCDE* RNA. Previous analysis (20) has shown that the kinetics of *cpeBA* and *cpeCDE* RNA accumulation are similar during transitions between RL and GL, which suggested that their expression might be controlled through a common mechanism. The data presented here clearly demonstrate that either different mechanisms or different combinations of mechanisms control the expression of these two operons. We have not yet determined whether CpeR controls transcription of *cpeBA* or acts posttranscriptionally. If CpeR does affect *cpeBA* transcription, our findings would be consistent with the apparent lack of any unique, highly conserved sequence motifs shared between the promoters of these two operons (20, 40, 42) and, together, these data would strongly suggest that their regulation primarily operates through different pathways. Our findings do not preclude the possibility that common aspects of the regulation of these operons exist.

The FdBk mutant was originally identified by its intermediate levels of accumulation of PC and PE in both RL and GL (25). In this study, our examination of *cpcB2A2*, *cpeBA*, and *cpeCDE* RNA levels in the FdBk revealed unexpected and significant differences in the RL- and GL-sensing mechanisms for these operons. Under the conditions used here, *cpcB2A2* RL- and GL-sensing occurs only through RcaE (Fig. 5D). The *cpeBA* operon is regulated primarily through RcaE (Fig. 5B), although the residual 7% RL and GL regulation represented a 2.9-fold level of GL induction. The RL-GL difference was statistically significant and observed in every experiment conducted. Thus, there is at least one additional system influencing the light quality responsiveness for this operon. Even more surprising was our finding that *cpeCDE* RNA levels were regulated by RL and GL at ca. 74% of the WT level (Fig. 5C). Thus, RcaE appears to have a relatively minor role in controlling the RL and GL responsiveness of the *cpeCDE* operon.

The residual threefold change in *cpeBA* transcript levels between RL and GL (Fig. 5B) might be expected to be visible in the FdBk mutant pigmentation phenotype. In fact, we occasionally observed slight variations in PE levels in this mutant (for example, see Fig. 1B), but typically these were no more than ca. 5% of the WT levels, a finding which correlates with the 7% RL-GL difference in *cpeBA* RNA levels in the FdBk mutant measured here (Fig. 5B). Since the linker proteins encoded by the *cpeCDE* operon are not chromophorylated, any RL versus GL differences in the abundance of these proteins in the FdBk mutant would not be visually detectable.

Because these findings constitute the first report of the *cpeBA* and *cpeCDE* operons being controlled by a light quality sensing system(s) other than that operating through RcaE, we carefully examined the FdBk mutant used in our studies for the presence of residual WT copies of *rcaE*. Both Southern blot (Fig. 6A) and PCR amplification approaches (Fig. 6B) identified only the form of *rcaE* containing the previously described DNA insertion in these cells (25). Western blot analysis of total protein from the FdBk mutant with anti-RcaE antibodies showed that no detectable RcaE is present in this mutant (Terauchi and Kehoe, unpublished). In addition, if any WT copies were present in the FdBk mutant, some difference in *cpcB2A2* expression might be expected, since both its activation and inactivation are more sensitive to RL-GL shifts than is *cpeBA* (33).

Our analysis of the FdTq1 mutant provides clear genetic evidence that the *cpeBA* and *cpeCDE* transcript accumulation is controlled, at least in part, through different mechanisms. Although the mechanism through which CpeR regulates *cpeBA* expression remains to be elucidated, its sequence similarity to the PP2C class of protein phosphatases provides a starting point for the testing of its function. In addition, the data presented here demonstrate that there is dramatic variation in the degree to which the RcaE-controlled system regu-

lates the RL and GL expression of the *cpcB2A2*, *cpeBA*, and *cpeCDE* operons. Collectively, these results clearly demonstrate that one or more important light-sensing mechanism(s), in addition to that controlled by RcaE, must regulate *cpeBA* and *cpeCDE* expression. The nature of the additional sensory system(s) that we have uncovered remains to be identified.

ACKNOWLEDGMENTS

We thank Rick Alvey, Lina Li, Barbara Quinby, Arthur Grossman, Bettina Kehoe, Beronda Montgomery, and Emily Stowe-Evans for their thoughtful reviews and comments.

This work was supported by startup funds from Indiana University and National Science Foundation grant MCB-0084297.

ADDENDUM IN PROOF

The altered patterns of *cpeBA* and *cpeCDE* transcript accumulation reported here for the FdTq1 mutant have also been found for a *cpeR* knockout mutant (J. Cobley, submitted for publication).

REFERENCES

1. **Allen, M. M.** 1968. Simple conditions for growth of unicellular blue-green algae on plates. J. Phycol. **4:**1–4.
2. **Altschul, S. F., T. L. Madden, A. A. Schäffer, J. Zhang, Z. Zhang, W. Miller, and D. J. Lipman.** 1997. Gapped BLAST and PSI-BLAST: a new generation of protein database search programs. Nucleic Acids Res. **25:**3389–3402.
3. **Altschul, S. F., W. Gish, W. Miller, E. W. Myers, and D. J. Lipman.** 1990. Basic local alignment search tool. J. Mol. Biol. **215:**403–410.
4. **Bakal, C. J., and J. E. Davies.** 2000. No longer an exclusive club: eukaryotic signaling domains in bacteria. Trends Cell Biol. **10:**32–38.
5. **Bennett, A., and L. Bogorad.** 1971. Properties of subunits and aggregates of blue-green algal biliproteins. Biochemistry **10:**3625–3634.
6. **Bennett, A., and L. Bogorad.** 1973. Complementary chromatic adaptation in a filamentous blue-green alga. J. Cell Biol. **58:**419–435.
7. **Bruns, B. U., W. R. Briggs, and A. R. Grossman.** 1989. Molecular characterization of phycobilisome regulatory mutants in *Fremyella diplosiphon*. J. Bacteriol. **171:**901–908.
8. **Bryant, D. (ed.).** 1994. The molecular biology of cyanobacteria. Kluwer Academic Publishers, Dordrecht, The Netherlands.
9. **Bryant, D. A.** 1981. The photoregulated expression of multiple phycocyanin species: general mechanism for control of phycocyanin synthesis in chromatically adapting cyanobacteria. Eur. J. Biochem. **119:**425–429.
10. **Campbell, D.** 1996. Complementary chromatic adaptation alters photosynthetic strategies in the cyanobacterium *Calothrix*. Microbiology **142:**1255–1263.
11. **Chang, C., S. F. Kwok, A. B. Bleecker, and E. M. Meyerowitz.** 1993. *Arabidopsis* ethylene-response gene *ERT1*: similarity of product to two component regulators. Science **262:**539–544.
12. **Chiang, G. G., M. R. Schaefer, and A. R. Grossman.** 1992. Complementation of a red-light indifferent cyanobacterial mutant. Proc. Natl. Acad. Sci. USA **89:**9415–9419.
13. **Chiang, G. G., M. R. Schaefer, and A. R. Grossman.** 1992. Transformation of the filamentous cyanobacterium *Fremyella diplosiphon* by conjugation or electroporation. Plant Physiol. Biochem. **30:**315–325.
14. **Cobley, J. G., and R. D. Miranda.** 1983. Mutations affecting chromatic adaptation in the cyanobacterium *Fremyella diplosiphon*. J. Bacteriol. **153:** 1486–1492.
15. **Cobley, J. G., E. Zerweck, et al.** 1993. Construction of shuttle plasmids which can be efficiently mobilized from *Escherichia coli* into the chromatically adapting cyanobacterium *Fremyella diplosiphon*. Plasmid **30:**90–105.
16. **Conley, P. B., P. G. Lemaux, and A. Grossman.** 1985. Cyanobacterial light-harvesting complex subunits encoded in two red light-induced transcripts. Science **230:**550–553.
17. **Conley, P. B., P. G. Lemaux, and A. Grossman.** 1988. Molecular characterization and evolution of sequences encoding light-harvesting components in the chromatically adapting cyanobacterium *Fremyella diplosiphon*. J. Mol. Biol. **199:**447–465.
18. **Das, A. K., N. R. Helps, P. T. W. Cohen, and D. Barford.** 1996. Crystal structure of the protein serine/threonine phosphatase 2C at 2.0 Å resolution. EMBO J. **15:**6798–6809.
19. **Diakoff, S., and S. Scheibe.** 1973. Action spectra for chromatic adaptation in *Tolypothrix tenuis*. Plant Physiol. **51:**382–385.
20. **Federspiel, N. A., and A. R. Grossman.** 1990. Characterization of the light-regulated operon encoding the phycoerythrin-associated linker proteins from the cyanobacterium *Fremyella diplosiphon*. J. Bacteriol. **172:**4072–4081.
21. **Federspiel, N. A., and L. Scott.** 1992. Characterization of a light-regulated gene encoding a new phycoerythrin-associated linker protein from the cyanobacterium *Fremyella diplosiphon*. J. Bacteriol. **174:**5994–5998.
22. **Fraser, C. M., et al.** 1995. The minimal gene complement of *Mycoplasma genitalium*. Science **270:**397–403.
23. **Haury, J. F., and L. Bogorad.** 1977. Action spectra for phycobiliprotein synthesis in a chromatically adapting cyanophyte *Fremyella diplosiphon*. Plant Physiol. **60:**835–839.
24. **Kahn, K., D. Mazel, J. Houmard, N. Tandeau de Marsac, and M. R. Schaefer.** 1997. A role for *cpeYZ* in cyanobacterial phycoerythrin biosynthesis. J. Bacteriol. **179:**998–1006.
25. **Kehoe, D. M., and A. R. Grossman.** 1996. Similarity of a chromatic adaptation sensor to phytochrome and ethylene receptors. Science **273:**1409–1412.
26. **Kehoe, D. M., and A. R. Grossman.** 1997. New classes of mutants in complementary chromatic adaptation provide evidence for a novel four-step phosphorelay system. J. Bacteriol. **179:**3914–3921.
27. **Kehoe, D. M., and A. R. Grossman.** 1998. Use of molecular genetics to investigate complementary chromatic adaptation: advances in transformation and complementation. Methods Enzymol. **297:**279–290.
28. **Kieber, J. J., M. Rothenberg, G. Roman, K. A. Feldman, and J. R. Ecker.** 1993. *CTR1*, a negative regulator of the ethylene response pathway in Arabidopsis, encodes a member of the Raf family of protein kinases. Cell **72:**427–441.
29. **Lomax, T. L., P. B. Conley, J. Schilling, and A. R. Grossman.** 1987. Isolation and characterization of light-regulated phycobilisome linker polypeptide genes and their transcription as a polycistronic mRNA. J. Bacteriol. **169:** 2675–2684.
30. **Maeda, T., S. M. Wurgler-Murphy, and H. Saito.** 1994. A two-component system that regulates an osmosensing MAP kinase cascade in yeast. Nature **369:**242–245.
31. **Mazel, D., G. Guglielmi, J. Houmard, W. Sidler, D. A. Bryant, and N. Tandeau de Marsac.** 1986. Green light induces transcription of the phycoerythrin operon in the cyanobacterium *Calothrix* 7601. Nucleic Acids Res. **14:**8279–8290.
32. **Mazel, D., J. Houmard, A. M. Castets, and N. Tandeau de Marsac.** 1990. Highly repetitive DNA sequences in cyanobacterial genomes. J. Bacteriol. **172:**2755–2761.
33. **Oelmüller, R., A. R. Grossman, and W. R. Briggs.** 1988. Photoreversibility of the effect of red and green light pulses on the accumulation in darkness of mRNAs coding for phycocyanin and phycoerythrin in *Fremyella diplosiphon*. Plant Physiol. **88:**1084–1091.
34. **Oelmüller, R., P. B. Conley, N. Federspiel, W. R. Briggs, and A. R. Grossman.** 1988. Changes in accumulation and synthesis of transcripts encoding phycobilisome components during acclimation of *Fremyella diplosiphon* to different light qualities. Plant Physiol. **88:**1077–1083.
35. **Oelmüller, R., A. R. Grossman, and W. R. Briggs.** 1989. Role of protein synthesis in regulation of phycobiliprotein mRNA abundance by light quality in *Fremyella diplosiphon*. Plant Physiol. **90:**1486–1491.
36. **Ohto, C., C. Ishida, H. Nakane, M. Muramatsu, T. Nishino, and S. Obata.** 1999. A thermophilic cyanobacterium *Synechococcus elongatus* has three different class I prenyltransferase genes. Plant Mol. Biol. **40:**307–321.
37. **Posas, R., S. M. Wurgler-Murphy, T. Maeda, E. A. Witten, T. C. Thai, and H. Saito.** 1996. Yeast HOG-1 MAP kinase cascade is regulated by a multistep phosphorelay mechanism in the SLN1-YPD1-SSK1 "two component" osmosensor. Cell **86:**865–875.
38. **Sambrook, J., E. F. Fritsch, and T. Maniatis.** 1989. Molecular cloning: a laboratory manual, 2nd ed. Cold Spring Harbor Laboratory, Cold Spring Harbor, N.Y.
39. **Schaefer, M. R., G. G. Chiang, J. G. Cobley, and A. R. Grossman.** 1993. Plasmids from two morphologically distinct cyanobacterial strains share a novel replication origin. J. Bacteriol. **175:**5701–5705.
40. **Schmidt-Goff, C. M., and N. A. Federspiel.** 1993. In vivo and in vitro footprinting of a light-regulated promoter in the cyanobacterium *Fremyella diplosiphon*. J. Bacteriol. **175:**1806–1813.
41. **Shi, L., M. Potts, and P. J. Kennelly.** 1998. The serine, threonine, and/or tyrosine-specific protein kinases and protein phosphatases of prokaryotic organisms: a family portrait. FEMS Microbiol. Rev. **22:**229–253.
42. **Sobczyk, A., G. Schyns, N. Tandeau de Marsac, and J. Houmard.** 1993. Transduction of the light signal during complementary chromatic adaptation in the cyanobacterium *Calothrix* sp. PCC 7601: DNA-binding proteins and modulation by phosphorylation. EMBO J. **12:**997–1004.
43. **Tandeau de Marsac, N.** 1977. Occurrence and nature of chromatic adaptation in cyanobacteria. J. Bacteriol. **130:**82–91.
44. **Tandeau de Marsac, N.** 1983. Phycobilisomes and complementary adaptation in cyanobacteria. Bull. Inst. Pasteur **81:**201–254.
45. **Tomioka, N., K. Shinozaki, and M. Sugiura.** 1981. Molecular cloning and characterization of ribosomal RNA genes from a blue-green alga, *Anacystis nidulans*. Mol. Gen. Genet. **184:**359–363.
46. **Vogelmann, T. C., and J. Scheibe.** 1978. Action spectrum for chromatic adaptation in the blue-green alga *Fremyella diplosiphon*. Planta **143:**233–239.